Sensitivity of a Mesoscale Model to Microphysical Parameterizations in the MAP SOP Events IOP2b and IOP8

STEFANO SERAFIN* AND ROSSELLA FERRETTI

Department of Physics/CETEMPS, University of L'Aquila, L'Aquila, Italy

(Manuscript received 20 July 2006, in final form 3 January 2007)

ABSTRACT

The sensitivity of a mesoscale model to different microphysical parameterizations is investigated for two events of precipitation in the Mediterranean region, that is, the Mesoscale Alpine Program (MAP) intensive observation periods (IOP) 2b (19–21 September 1999) and 8 (20–22 October 1999). Simulations are performed with the fifth-generation Pennsylvania State University–National Center for Atmospheric Research Mesoscale Model (MM5); the most commonly used bulk microphysical parameterization schemes are evaluated, with a particular focus on their impact on the forecast of rainfall. To evaluate the forecast skill, the verification is carried out quantitatively by using the observations recorded by a high-resolution rain gauge network during the MAP campaign. The results show that, for the surface rainfall forecast, all microphysical schemes produce a similar precipitation field and none of them perform significantly better than the others. The ability of different schemes to reproduce events with different ongoing microphysical processes is briefly discussed by comparing model simulations and knowledge of hydrometeor fields from radar observations. The vertical profiles of hydrometeors from two of the analyzed schemes show gross similarities with available radar observations. Last, the role of one of the parameterizations appearing in a typical bulk microphysical scheme, that is, the one of the snowfall speed, is evaluated in detail. Adjustments in the semiempirical relationships describing the fall speed of snow particles have a large impact, because a reduced snowfall speed enhances precipitation on the lee side of mountain ridges and diminishes it on the windward side. Anyway, this effect does not appear to be able to largely improve or reduce the forecast skill of the MM5 systematically; the impact of changes in the parameterization of the snow deposition velocity very likely depends on the dynamics of the event under investigation.

1. Introduction

A high-resolution numerical forecast of rainfall in a region with complex orography is seldom successful; under- or overestimation of precipitation, and phase or position errors are common in mesoscale models with a resolution of a few kilometers (Brewster 2003). The role of microphysical schemes is only recently being addressed as a potential problem in this context. Several studies have been performed using different and complex microphysical parameterizations, addressing the issue of errors in both the location and intensity of the modeled rainfall field. Gilmore et al. (2004) evaluated the impact of a few different bulk microphysical schemes on the precipitation production rate and on the low-level cooling rate using a 3D nonhydrostatic cloud model. They found that the rainfall production almost doubled when schemes that include parameterized ice-phase processes were used. Lynn et al. (2005a,b) investigated the sensitivity of rainfall to a novel spectral bin microphysical scheme coupled with the fifth-generation Pennsylvania State University–National Center for Atmospheric Research (NCAR) Mesoscale Model (MM5; Dudhia 1993; Grell et al. 1994). They found a remarkable improvement in the rainfall forecast with respect to other bulk parameterizations, but the computing time needed by the new scheme did not allow for its operational implementation. An investigation of the role of microphysical parameterizations in determining location errors in the precipitation forecast has been carried out by Colle et al. (1999), who studied the sensitivity of the rainfall rate

* Current affiliation: Department of Civil and Environmental Engineering, University of Trento, Trento, Italy.

Corresponding author address: Rossella Ferretti, Dept. of Physics/CETEMPS, University of L'Aquila, Via Vetoio, L'Aquila 67010, Italy.
E-mail: rossella.ferretti@aquila.infn.it

DOI: 10.1175/JAM2545.1

to different parameterizations of the fall speed of snowflakes, always using the MM5. They showed a large underestimation of precipitation in the lee of a mountain ridge, which was partially recovered by reducing the snowfall speed. Colle and Zeng (2004) established a relationship between the width of mountain barriers and the features of microphysical processes, suggesting that there is a large variability of the microphysics parameters depending on the geographical area. Lynn et al. (2005a) and Colle et al. (2005) also investigated the impact of the deposition velocity of snowfall on the forecast of rainfall, as well as its dependency on the topography and geographical area.

A field campaign called Improvement of Microphysical Parameterization through Observational Verification Experiment (IMPROVE)-2 was recently held over the Oregon Cascade Mountains, with the aim of obtaining comprehensive measurements of cloud microphysical variables for various precipitation events. The collected data are suitable for a comparison between observations and model forecasts, and offer the opportunity to improve bulk microphysical parameterizations in mesoscale models (Stoelinga et al. 2003). In various IMPROVE-2 events, a comparison between the measured and modeled distributions of the size of snow particles suggested that key factors to obtaining a successful forecast of precipitation are the intercept of the snow size distribution and the total mass concentration of snow particles. An excessive mass concentration of snow aloft produced an overestimation of the precipitation to the lee of the Cascade Range (Garvert et al. 2005); the authors suggested as a possible source of this error the temperature-dependent intercept used in their model. The impact of the parameterization of riming was instead studied by Colle et al. (2005), who concluded that a simple warm-rain scheme produced the lowest mean error if compared with schemes including ice-phase processes.

Ferretti et al. (2003) and Rotunno and Ferretti (2003) reported an underestimation of rainfall over complex terrain by MM5 in the Mediterranean area where, similarly to what happens in the northwestern United States, air masses interact with several mountain ridges that are characterized by variable width and closeness to the sea. Based on the studies cited so far, this work investigates whether the impact of microphysical schemes on MM5 simulations is as relevant in the Mediterranean region as it is in the U.S. Pacific Northwest. The dataset collected during the field campaign of the Mesoscale Alpine Program (MAP; Bougeault et al. 2001) is used for the purpose. Several intensive observation periods (IOPs) affected by rainfall were observed on both sides of the Alps between September and November 1999, and during two of them (IOP2b and IOP8) most operational models failed in forecasting rainfall over the Po Valley. These are chosen as test cases for this study.

The main problems addressed here are as follows:

1) We hope to understand whether MM5, in a configuration suitable for operational forecasting, is able to capture differences in microphysical processes in IOP2b and IOP8, given its ability to correctly reproduce their different dynamical features. The conceptual model of precipitation-forming processes proposed by Medina and Houze (2003), based on measurements taken in the two events by a polarimetric radar, is used as a term of comparison;
2) We hope to understand how much of the error in precipitation location and amount depends on the parameterization of microphysics and on one feature in particular, that is, the formulation of the snowfall speed. The interest in this particular detail of bulk microphysical schemes stems from previous investigations reporting its relevant impact in a meteorological and geographical context different from the Mediterranean area, for example, the already cited works by Lynn et al. (2005a) and Colle et al. (2005). It is expected that using microphysical schemes that include ice-phase processes has an impact on the forecast of surface rainfall, while tuning the snowfall speed parameterization might alter the spatial distribution of rainfall areas.

To address the two issues mentioned above, three different microphysical schemes are compared using standard verification scores, and sensitivity experiments to the snow deposition velocity are performed. Depending on the results of this work, detailed investigations of how other particular aspects of bulk microphysical schemes that include the rainfall forecast, and of the way bulk microphysical schemes may be improved in order to achieve a better representation of real world processes, may follow this study.

The paper is organized as follows. In section 2 the main meteorological characteristics of the two events are presented. A description of the model setup for numerical simulations is provided in section 3, along with details on the microphysical schemes used. Section 4 explains results related to the sensitivity to microphysical schemes and snowfall speed parameterizations. Conclusions are drawn in section 5.

2. The cases: IOP2b and IOP8

The MAP campaign was conventionally divided into IOPs—IOP2b started at 0000 UTC 19 September and

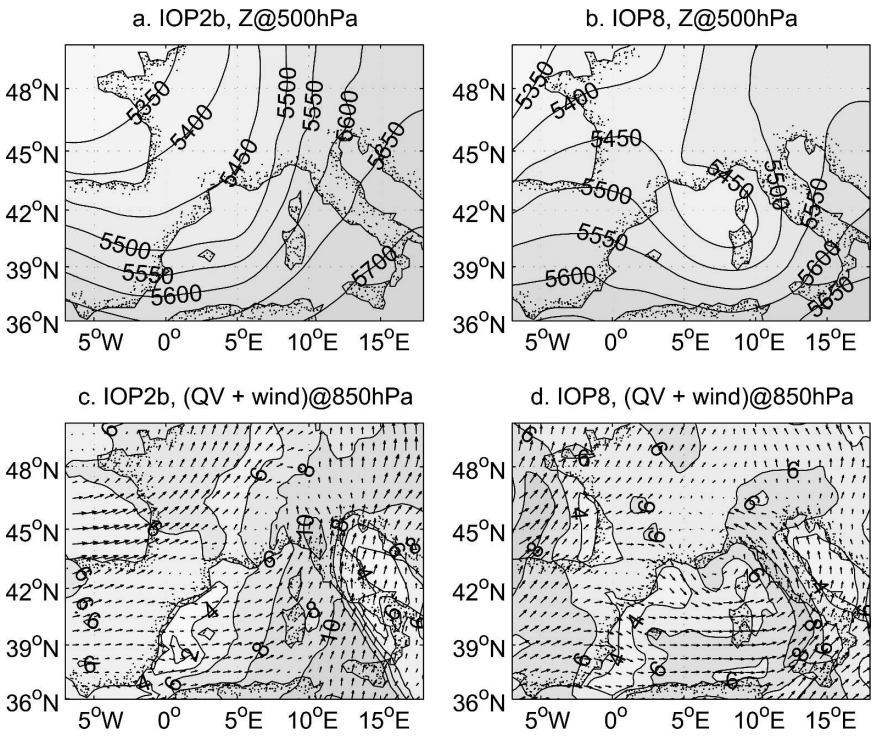

FIG. 1. ECMWF analyses showing 500-hPa geopotential height, and horizontal wind vectors and specific humidity at 850 hPa for (a), (c) IOP2b at 1200 UTC 20 Sep 1999 and for (b), (d) IOP8 at 1200 UTC 21 Oct 1999.

ended at 0000 UTC 21 September 1999 and IOP8 started at 0000 UTC 20 October and ended at 0600 UTC 22 October 1999. Forecasters (and models) deemed the synoptic situation of both events favorable for the occurrence of heavy rainfall.

The dynamical features of the two events, and the ability of several models (among them MM5) to correctly reproduce them, have already been discussed in a quantity of recent contributions. The dynamics, moisture, and large mesoscale aspects that differentiate the two cases were discussed by Rotunno and Ferretti (2003) using simulations with MM5. A further investigation and verification of the evolution of the large mesoscale forcing in IOP2b, and its relationship with the forecast of precipitation, was performed by Faccani and Ferretti (2005) and Ferretti and Faccani (2005). The verification of MM5 simulations at a 9-km resolution in all MAP wet IOPs was presented by Ferretti et al. (2003). A comparative analysis of the performance of different models in simulating rainfall in IOP2b was also provided by Richard et al. (2002). Building on this wide body of literature, the work herein only briefly summarizes the most distinctive characters of the two events and refers to the relevant sources whenever appropriate.

Typical factors determining severe precipitation in the Mediterranean region are the presence of moisture-laden air over the sea, and a meridional southerly flow blowing the humid air toward mountain ridges (Doswell III et al. 1998). During both IOP2b and IOP8 a deep trough at 500 hPa approached northern Italy from the west. The circulation induced by the trough advected humid air above the Mediterranean Sea toward northwestern Italy, interacting with two different orographic obstacles: the Ligurian Apennines and the Alps. The freezing level was located at about 3000 and 2500 m above sea level, respectively, for IOP2b and IOP8.

Despite the similar large-scale circulation, the two events featured different local flows, as noticed by Rotunno and Ferretti (2003). IOP2b was characterized by a low-level southerly flow, turning southeasterly approaching the Alpine ridge (Fig. 1a). Thus, airflow was perpendicular to the direction of the mountain barrier. On the other hand, IOP8 was characterized by low-level southern winds with a strong easterly component over the Po Valley, which rotated counterclockwise over the Piedmont region along the mountain barrier (Fig. 1b). The southern wind blowing from the Mediterranean Sea could not reach the Alps in this case, because it was deflected west by the Liguria Apennines. Medina et al. (2005) highlighted how the weather dy-

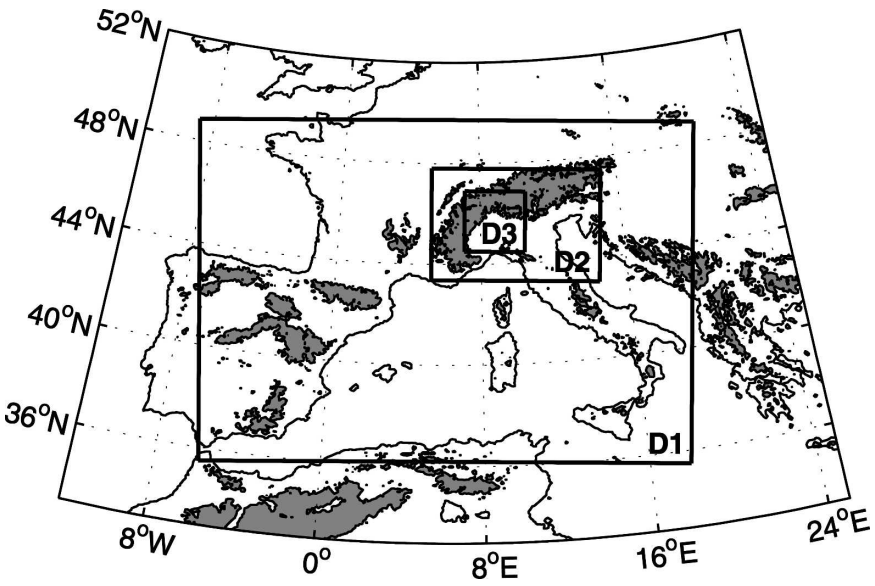

FIG. 2. The model domains and terrain elevation: D1, D2, and D3 have a grid spacing of 27, 9, and 3 km, respectively. The shaded areas delimit regions with altitude greater than 1000 m.

namics for the IOP8 MAP case share some common features with the IMPROVE-2 Oregon Cascade storm (13–14 December 2001). Both events were characterized by a baroclinic system approaching the mountain barrier (the Alps in one case, and the Oregon Cascade Range in the other) and a preexisting stable stratified upstream flow; precipitation on the windward side of the ridges were observed in both cases.

The areal distribution and intensity of rainfall produced by the different flow regimes in IOP2b and IOP8 are different. The observed precipitation (see Rotunno and Ferretti 2003, their Fig. 4) shows that during IOP2b rainfall was restrained mainly on the windward (southern) slopes of the Alps. The average accumulated rainfall was greater than 100 mm day^{-1} over both Piedmont (west Po Valley) and Friuli (east Po Valley); it reached a peak value of 351 mm day^{-1} in Piedmont, and it also extended well beyond the Alpine ridge over Switzerland. In comparison, during IOP8 rainfall was widespread over the plains of the Po Valley, and was much less intense (60 mm day^{-1} at most). In a study by Rotunno and Ferretti (2003), MM5 correctly recognized the main differences between the two cases: flow-over (IOP2b) versus flow-around (IOP8) airflow regimes, as well as the moderate (IOP2b) versus light (IOP8) rainfall.

Medina and Houze (2003) analyzed the microphysical processes and rainfall patterns occurring in the two events, and found some remarkable differences. The blocked case (IOP8) was characterized by purely stratiform precipitation, in which the most relevant processes were the homogeneous growth of ice and cloud water particles by water vapor diffusion, the aggregation of ice particles to form snowflakes, and the melting of snow to form rain. In the unblocked case (IOP2b), the low static stability of the atmosphere favored the development of orographic uplifting cells and the onset of convection in the late afternoon of 20 September 1999 (Medina and Houze 2003; Rotunno and Ferretti 2003). The forced ascent of air masses resulting from convective motions produced a large amount of supercooled liquid water above the 0°C isotherm, and thereby enhanced the processes of riming and creation of graupel and hail in the cells.

3. Numerical experiments

a. Model configuration

MM5, version 3.7 (V3.7), a nonhydrostatic model utilizing the primitive equations (Dudhia 1993; Grell et al. 1994), is adopted for this study. Three two-way-nested domains are used to enhance resolution over northern Italy. The mother domain is centered at 42.95°N, 6.05°E, with a 27-km grid spacing. The second and third domains have 9- and 3-km grid spacing, respectively. The second domain is located over northern Italy, and the third one encompasses the Lago Maggiore target area (Fig. 2). The model simulations are performed using 29 unequally spaced terrain-following vertical levels. They last from 1200 UTC 19 September to 1200 UTC 21 September 1999 for IOP2b, and from 1200 UTC 20 October to 1200 UTC 22 October 1999 for IOP8. The European Centre for Medium-Range

Weather Forecasts (ECMWF) analyses for temperature, wind speed, relative humidity, and geopotential height on 11 mandatory pressure levels are interpolated to the MM5 horizontal grid and to sigma levels to produce the model initial and boundary conditions.

The Kain–Fritsch scheme (Fritsch and Kain 1993) for cumulus convection (domains 1 and 2 only), the Medium-Range Forecast (MRF) scheme for the PBL (Hong and Pan 1996) and the MM5 cloud–radiation scheme for radiative transfer (Dudhia 1993; Grell et al. 1994) are used. To evaluate the impact of microphysics on the model rainfall, three different microphysical schemes are analyzed: the Reisner "mixed phase" (R1) scheme (Grell et al. 1994), the Goddard Space Flight Center (G) GCM model microphysical scheme (Tao and Simpson 1993), and the Reisner "graupel included" (R2) scheme (Reisner et al. 1998) with the snow intercept parameter depending on temperature (Thompson et al. 2004).

A test run has been performed using a further high-resolution (1 km) model domain, two-way nested in a small region included in domain 3. This fourth domain was located in an area on the southern slope of the Alps in proximity to the Po Valley, in order to better resolve the orographic uplifting of air masses and quantify the impact of the increased resolution on the rainfall forecast. As expected, the results show that the rainfall volume produced in domains 2, 3, and 4 in the region where they overlap does not vary considerably, although localized peaks of intense precipitation were produced in the domain with the highest resolution (not shown). Therefore, we conclude that, for our purpose, we can rely on the two-way-nesting properties of MM5, and that a maximum resolution of 3 km is enough to capture properly the effect of mountain forcing on precipitation. Moreover, a series of numerical experiments are performed to test the sensitivity of the model precipitation to the fall speed of snow. In the following sections the differences between these microphysical schemes and between some available empirical formulas for the snowfall speed are briefly discussed.

b. Microphysical schemes

Simplified microphysical schemes for operational mesoscale weather prediction models generally account for four different water categories, that is, cloud water q_c, cloud ice q_i, rain q_r, and snow q_s. Among the microphysical parameterizations available for MM5, the R1 scheme allows for cloud ice, cloud water, and rain to be produced simultaneously, but it does not account for the production of graupel or hail. Instead, both the R2 and G schemes include one further prognostic equation for graupel q_g. In all the above schemes it is assumed that the dimensional distribution of the hydrometeors is exponential (Marshall and Palmer 1948):

$$N_h dx = N_h^0 e^{-\lambda x} dx, \tag{1}$$

where h is a generic hydrometeor (r, s, or g for rain, snow, or graupel, respectively), N_h is its number concentration, x is the particle size, λ is the slope parameter, and N_h^0 is a parameter describing the intercept of the distribution. Here, λ is inversely proportional to the mixing ratio of the hydrometeor q_h:

$$\lambda = \left(\frac{\pi \rho_h N_h^0}{\rho q_h} \right)^{1/4}, \tag{2}$$

where ρ is the density of air and ρ_h is the hydrometeor density. Thus, the greater the mixing ratio is, the wider is the size distribution. The intercept parameters N_h^0 are fixed in the R1 and G schemes, whereas two prognostic equations account for N_s^0 and N_g^0 in the R2 scheme (a two-moment scheme). The three schemes differ in the constants describing the density and number concentration of hydrometeors, as summarized in Table 1, and most remarkably in the parameterization of conversion processes between different hydrometeor species (see the R1, R2, and G references for details).

TABLE 1. The intercept parameters of the Marshall–Palmer size distributions and the densities of hydrometeors used in the R1, R2, and G microphysical schemes.

	R1	R2	G
N_r^0	8×10^6 m^{-4}	8×10^6 m^{-4}	8×10^6 m^{-4}
N_s^0	2×10^7 m^{-4}	Predicted	4×10^6 m^{-4}
N_g^0	Missing	Predicted	4×10^6 m^{-4}
ρ_r	1000 kg m^{-3}	1000 kg m^{-3}	1000 kg m^{-3}
ρ_i	500 kg m^{-3}	500 kg m^{-3}	917 kg m^{-3}
ρ_s	100 kg m^{-3}	100 kg m^{-3}	100 kg m^{-3}
ρ_g	Missing	400 kg m^{-3}	400 kg m^{-3}

c. Snowfall speed

An interesting aspect of microphysical parameterization schemes is the representation of the deposition velocity of precipitating particles. This study is specifically focused on the parameterization of the fall speed of snowflakes. This choice is made because snowflakes are much less dense than raindrops, and therefore snow tends to be advected more effectively by the prevalent wind, exerting a large impact on the spatial structure of the modeled rainfall field.

Two simple hypotheses are usually invoked in order to describe the behavior of precipitating particles in a parsimonious way. The first assumption is the aforementioned Marshall–Palmer (exponential) distribution

for the size distribution of particles; the second one is that the fall velocity is related to the diameter of a precipitating particle through a simple power law ($V = aD^b$). Using these hypotheses, the mass-weighted terminal velocity of hydrometeors V may be expressed as

$$V = \frac{a\Gamma(4 + b)}{6\lambda^b}. \quad (3)$$

This estimate of the average fall speed is then used to compute the precipitation terms in the prognostic equations for the mixing ratios of hydrometeors.

In particular, the law for the snowfall speed used by MM5 (denoted by LH) is the one proposed by Locatelli and Hobbs (1974):

$$V_{\mathrm{LH}} = 11.72D^{0.41}, \quad (4)$$

where V is the fall speed of a snow particle (m s^{-1}) and D is its diameter (m). Colle and Mass (2000) suggested using the fall speed, denoted by C,

$$V_C = 16.78D^{0.527}, \quad (5)$$

which describes more closely the deposition of unrimed radiating assemblages of dendrites (Cox 1988). This last power law produces a smaller fall speed than LH for a given particle diameter, and it is thus expected to favor the advection of precipitating particles past orographic obstacles. Colle and Mass (2000) obtained 10%–20% less precipitation on windward slopes and 10%–60% more on lee slopes of the flow when using C instead of LH. Moreover, they noticed an increase in the model bias and a slight decrease in the root-mean-square error at high precipitation rates. In their study, enhancing precipitation on lee slopes was enough to obtain an improvement in the overall rainfall forecast. On the other hand, Colle at al. (2005) reported an opposite effect for an IMPROVE-2 event: the C law deteriorated the precipitation forecast on the lee of a ridge.

Other such semiempirical relationships can be found in common textbook references (e.g., Pruppacher and Klett 1997). For instance, we cite the two formulas by Jiusto and Bosworth (1971):

$$V_{\mathrm{JB1}} = 2.71D^{0.206} \quad \text{and} \quad V_{\mathrm{JB2}} = 3.95D^{0.206}, \quad (6)$$

which describe, respectively, aggregates of dendrites and plates (JB1) and aggregates of columns (JB2), and the two by Davis (1974):

$$V_{D1} = 43.55D^{0.748} \quad \text{and} \quad V_{D2} = 3.23D^{0.442}, \quad (7)$$

the former of which is valid for platelike ice crystals with diameters ranging from 10 to 1000 μm, and the latter for bigger particles (500–3000 μm). All of the above formulas assume V in meters per second and D in meters. The shapes of the various V/D relationships are shown in Fig. 3.

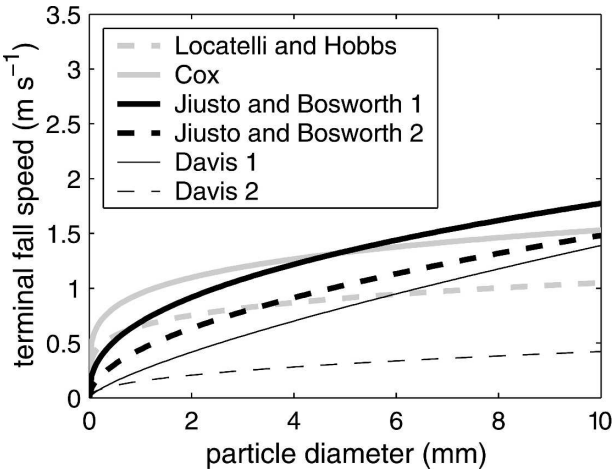

FIG. 3. Empirically derived relationships between deposition velocity and particle diameter.

In bulk microphysical schemes no distinction is usually made between different snowflake categories, and the parameterization of the snowfall speed is tuned on only one representative snowflake type. Given the large differences existing in the terminal fall speeds of different snow crystals, as illustrated by Eqs. (4)–(7), the issue of deciding from time to time which snowflake type and V/D relationship should be taken as being representative is nontrivial. In this study, the quantitative effect of some of the possible choices is evaluated to assess the impact that this particular parameterization has on the estimation of rainfall.

Anyway, it has to be noticed that tuning the a and b coefficients in the V/D relationship is not the only way to affect the model-computed hydrometeor fall speeds. The calculated terminal fall velocity of the precipitating particles also depends on other assumptions about their size distribution. In particular, the slope parameter λ may play an important role in determining the fall velocity, and as a consequence the location of precipitation. A value of λ that is too small would result in a fall speed that is too high and in precipitation shadowing on the lee sides of mountain ridges. The same remark can be made about N_h^0, considering that λ is directly proportional thereto. Sensitivity tests to N_s^0 (for snow particles) were performed by Colle et al. (2005); they showed how the introduction of a temperature-dependent parameterization for N_s^0 did not produce a significant improvement to their simulations.

d. Numerical experiments

In light of the preceding discussion about microphysical schemes and the parameterization of the snowfall

TABLE 2. The experiments performed using different microphysical schemes and snowfall speed parameterizations.

Experiments	IOP2b	IOP8	Microphysics scheme	Fall speed
R1CNTR	*	*	R1	Locatelli and Hobbs (1974)
R1COX	*		R1	Cox (1988)
R1D2	*		R1	Davis (1974)
R2	*	*	R2	–
G	*	*	G	–

speed, several numerical experiments have been performed. The first aim stated in the introduction (i.e., understanding whether mesoscale simulations with MM5 may provide a reliable reproduction of microphysical conditions, discriminating between events with different microphysical processes) is pursued by comparing simulations for the two test cases of IOP2b and IOP8 with the three available schemes R1, R2, and G. The second point (i.e., evaluating the impact of the parameterization of the deposition velocity of the snow) is instead addressed by performing different runs for IOP2b, using the R1 scheme, and evaluating different formulations of the fall speed relationship (the LH, C, and D2 formulas). Table 2 summarizes the different numerical experiments performed.

e. Verification scores and root-mean-square error

Common verification indices (skill scores and root-mean-square error) are used as objective methods to compare model experiments for the two test cases. Here we assume that validated rain gauge data offer an accurate description of the true precipitation field, which is quite a strong hypothesis considering that a sample of scattered point measurements is seldom representative of a very intermittent phenomenon like rainfall. However, a bilinear interpolation of the gridded model data to the coordinates of measurement stations is performed, and the data of all rain gauges available during the MAP campaign for IOP2b and IOP8 are used. A large number of measurements is necessary to compute meaningful scores, and therefore the analysis is performed on the model domain 2, which includes a larger number of rain gauges than domain 3. Extending the analysis to domain D2 also allows for detection of whether spatial variations in the model skill occur, which would not be possible using data from domain D3 only (which is located in a small and geographically homogenous region, completely included in the windward side of the Alps). The choice to not use the simulations of the domain with highest resolution for the purpose of verification may seem counterproductive, but it is easily justified considering that D2 has an area of approximately 340 000 km^2, and that it contains a total of 546 measurement points. This implies that every rain gauge is, on average, representative of an area of about 25 km $\times$ 25 km, which is similar to the effective resolution of the model in D2. Moreover, the three domain runs used in this study provide a reliable representation of the interaction of the atmospheric flow with the mountain barrier (simulations of D3 affect all meteorological parameters of D2 because of the two-way nesting capability of MM5).

Although verification scores are supposed to give significant information about the systematic behavior of a particular model only if computed on a collection of many events, we believe that useful indications can be obtained from the analysis of the bias score (bias) and equitable threat score (ets) even on small time scales (48 h). In this particular context, the high density of rainfall measurements in space and time will compensate for the availability of very short time series.

The bias score allows for assessment of the over- or underestimation of the precipitation above a certain threshold, although it bears no information about the correspondence between single forecasts and observations. In general, bias greater than one indicates overforecasting, whereas bias less than one is indicative of underforecasting. On the other hand, the ets roughly quantifies the percentage of correct forecasts that can be ascribed to the model skill (i.e., the percentage of nonrandom correct forecasts), with values ranging from slightly negative (forecast worse than random) to 1 (perfect forecast). See Wilks (1995) or Jolliffe and Stephenson (2004) for a thorough description of various indices used in forecast verification.

The root-mean-square error (rmse) of the model rainfall is also used to evaluate the model error for each simulation. Two indices were defined: a global rmse and a station-specific rmse$_i$. The former accounts for t hourly rainfall forecasts and observations (f and o) at N available stations, and it is used as an overall evaluation parameter for the model forecast:

$$\mathrm{rmse} = \frac{Nt}{\sum_{i=1}^{N}\sum_{j=1}^{t} o_{ij}}\left[\frac{1}{Nt}\sum_{i=1}^{N}\sum_{j=1}^{t}(f_{ij}^2 - o_{ij}^2)\right]^{1/2}. \quad (8)$$

The latter is simply the rmse computed at every single measurement station:

$$\mathrm{rmse}_i = \frac{t}{\sum_{j=1}^{t} o_j}\left[\frac{1}{t}\sum_{j=1}^{t}(f_j^2 - o_j^2)\right]^{1/2}. \quad (9)$$

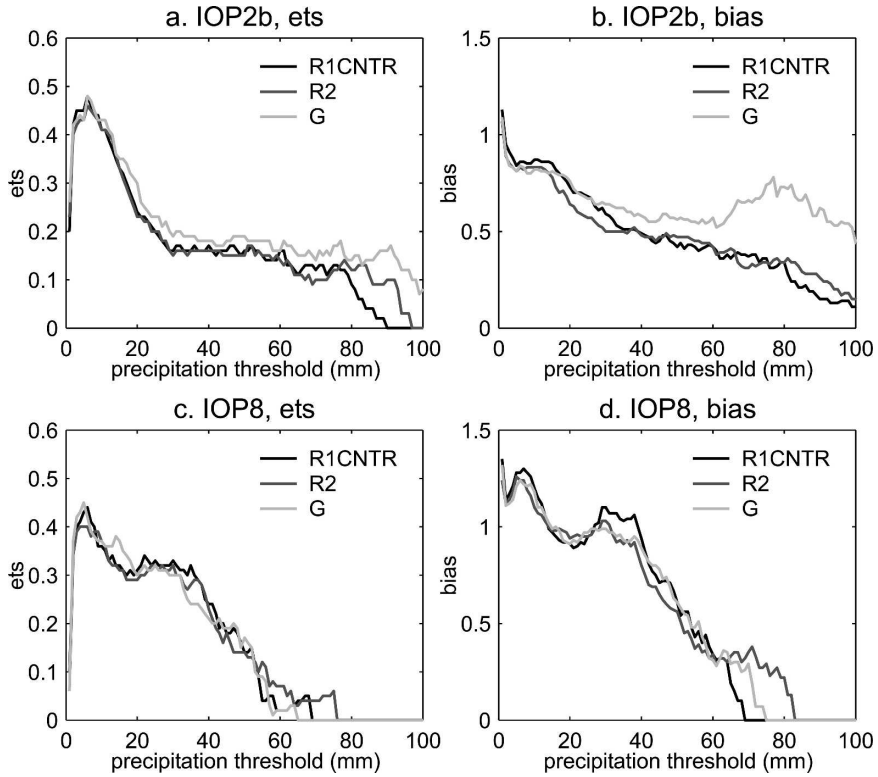

FIG. 4. (a), (c) Ets and (b), (d) bias for the 12-h rainfall for (top) IOP2b and (bottom) IOP8. The results of different simulations are represented by a gray color scale: R1CNTR, black; R2, dark gray; and G, light gray.

Both indices are normalized by scaling the rmse to the average value of the observed precipitation, to make them sensitive to the relative magnitude of the model error. This allows for a comparison of the model error in different precipitation regimes. As an example, forecasts in mountain regions usually show high rmse_i, but this may be related to higher precipitation rates rather than to bad model performance. Scaling on the average precipitation allows for a correct assessment of such situations.

4. Results

a. Verification scores: Bias, ets, and rmse

Verification scores are presented for IOP2b and IOP8 for the simulations R1CNTR, R2, and G. These are computed from a comparison of observed and forecast precipitation at all available stations inside domain D2 (a total of 546 points of measurement) using 12-h rainfall totals. As found by previous investigators (Rotunno and Ferretti 2003; Ferretti and Faccani 2005), MM5 underestimates heavy precipitation in both test cases. This is confirmed by the runs performed in this study (see the bias score; Figs. 4b,d).

Both ets and bias reach a zero value at lower rainfall rates in IOP8 than those in IOP2b, because the former event was characterized by lighter precipitation than the latter. The ets shows (Figs. 4a,c) a peak value reaching approximately 0.45–0.5 in both IOPs for rainfall thresholds less than 10 mm, whereas it decreases rapidly at higher thresholds. The forecast for IOP8 appears to be more skilful than that for IOP2b at intermediate rainfall amounts, with an ets reaching from 0.3 up to 40 mm of precipitation. The simulations for IOP8 appear to be more realistic, providing a correct forecast of the occurrence of precipitation (bias close to 1) up to 40-mm thresholds, as compared with 20 mm for IOP2b. Ferretti et al. (2003) obtained slightly better scores for bias and ets in an analysis of all the wet IOPs of the MAP campaign. Anyway, the verification statistics obtained in this work appear to be overall in good agreement with previous studies.

Turning now the attention on the effect of the representation of microphysical processes, the key point emerging from the examination of Fig. 4 is that a moderate variability among simulations with different microphysical schemes is only found at large precipitation thresholds: different microphysical schemes do not

TABLE 3. The scaled root-mean-square error for the MM5 precipitation forecasts for IOP2b and IOP8, using different microphysical schemes and different accumulation periods.

Root-mean-square error						
	IOP2b			IOP8		
	R1	R2	G	R1	R2	G
1 h	3.25	3.23	3.30	2.56	2.55	2.67
6 h	2.59	2.60	2.58	1.74	1.77	1.79
12 h	1.94	1.95	1.94	1.35	1.39	1.36
24 h	1.76	1.76	1.74	1.09	1.14	1.10
48 h	1.29	1.30	1.25	0.82	0.86	0.82

have significantly different scores at weak rainfall rates—neither in IOP2b nor in IOP8. Model skill appears to be affected by the choice of microphysical schemes only at very high precipitation amounts, where the adoption of the graupel water category seems to be beneficial to the forecast in convective conditions—in particular, during IOP2b (see the curves for the R2 and G schemes having a higher ets, and a bias closer to 1).

The analysis of the root-mean-square error (Table 3) provides results that are in line with those obtained by evaluating the verification scores. The global errors for the different model configurations, computed using the whole set of available stations, suggest that the model error for IOP8 is always less than that for IOP2b, and that the R1, R2, and G schemes give similar results for all of the model runs. Therefore, the choice of the microphysical scheme does not seem to affect the skill of model forecasts at this time scale, which ranges from 1 h to 2 days. Table 3 also shows that the global error decreases as the accumulation time period increases. This is expected because testing the model with respect to 48-h accumulated precipitation allows for a certain level of time uncertainty in the forecast, which is not allowed if using hourly precipitation.

b. Spatial distribution of ets, bias, and rmse

The hourly precipitation data are used to compute the spatial distribution of the verification indices. In what follows only the R1CNTR simulations for IOP2b and IOP8 are analyzed, because no remarkable differences are detected among experiments using other microphysical schemes. The score discrimination threshold used to compute ets and bias is set to 0.3 mm to examine the model ability to predict the occurrence or absence of precipitation in one place at a given time. The distribution of verification scores is displayed in Fig. 5.

The areal distribution of ets suggests (Figs. 5a,d) large spatial variations in the model skill in both test cases: high ets values are found in southeastern France and northeastern Italy for IOP2b (Fig. 5a), and in the Piedmont region for IOP8 (Fig. 5d). On the other hand, the lowest ets is found in the Piedmont region for IOP2b and in northeastern Italy for IOP8. Low values of the ets are also found on the lee (northern) side of the Alpine ridge for IOP2b, as well as on the alpine ridge between France and Piedmont for IOP8.

The analysis of the areal distribution of bias for IOP2b reveals a large underestimation of rainfall in the Piedmont and Lombardy plains (Fig. 5b, dark dots), whereas a small overestimation of the rainfall is found in the mountains and in the northeastern Po Valley. A different tendency is found for IOP8: a large overestimation is found along the highest ridges in the Alps (Fig. 5e, white dots), whereas a small underestimation is found in the plains (Fig. 5e, dark dots).

The areal distribution of the normalized rmse_i (Figs. 5c,f) has features similar to those of the previous scores. The rmse_i shows high values along the Po Valley and low values in the mountains (especially in the western part of the domain) for IOP2b; on the contrary, for IOP8 the lowest model errors are gathered in central northern Italy and in southern France, whereas the highest values are reached in mountain areas, particularly on the lee side of the Alps.

On the overall, these results suggest that MM5 has a tendency to trigger precipitation only if strong uplifting occurs, resulting from, for instance, either the presence of mountain ridges or strong synoptic forcing—for example, related to the presence of a frontal system. This clearly results from the high ets achieved over southern France for IOP2b, where the precipitation was stratiform and related to frontal uplifting, or by the high bias commonly observed over the mountains, where orographic lifting occurs in both IOP2b and IOP8. In particular, the scores for the two events suggest that the MM5 tends to be too dry in the plains for IOP2b and too wet in the mountains for IOP8. This agrees well with Ferretti et al. (2003), who clearly showed underestimation of precipitation in the Po Valley by MM5. Shortcomings in the forecast of rainfall may be related either to the particular flow characteristics or to unrealistic initial conditions, as shown by Faccani and Ferretti (2005) for IOP2b.

Although it is not shown in Fig. 5, it is easily realized that microphysical schemes do not affect the areal distribution of verification scores. This happens because the rainfall threshold used to evaluate this distribution is small, and falls in a range where the model skill is practically independent of the choice of microphysical

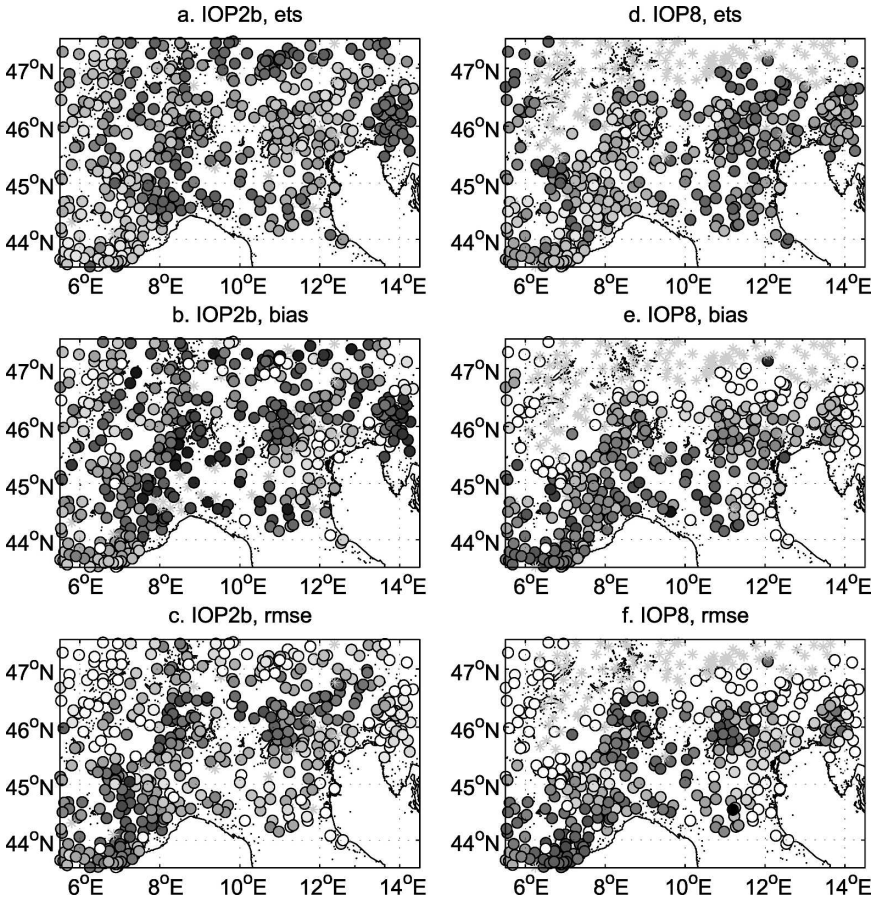

FIG. 5. Areal distribution of (a), (d) ets, (b), (e) bias, and (c), (f) rmse_i for the R1CNTR runs for IOP2b and IOP8, respectively. Ets and bias are calculated from hourly precipitation, with a threshold of 0.3 mm. Rmse_i is calculated from hourly model data and scaled on averaged local hourly precipitation. Circles with different shades of gray represent different values of verification indices. Ets ranges from 0 (black, worse) to 1 (white, best); bias less than 1 (underestimation) is shown by dark dots while bias greater than 1 (overestimation) corresponds to light dots; a null rmse_i is represented by black dots, while increasingly higher errors are shown by lighter shades of gray. Stars correspond to undefined values of the indices (either for the unavailability of measurements or for the absence of rainfall).

parameterization (as was explained in the previous paragraph).

c. *Vertical profiles of model-predicted hydrometeor mixing ratios*

An analysis of the average vertical distribution of different hydrometeors produced by MM5 using the R1, R2, and G schemes on domain 3 (3 km) is now presented: vertical profiles of the mixing ratios of hydrometeors produced by the three schemes are averaged in time (48 h) and space (all of domain 3). As already pointed out (section 3a), no parameterization of convective processes has been used in the simulation of D3, and consequently the hydrometeor fields presented here are the result of the interaction of microphysical schemes with explicitly resolved convection. Moreover, it is verified through the four-domains run (a maximum resolution of 1 km) that the vertical distributions of hydrometeors are not appreciably resolution dependent if averaged in space and time; that is why a minimum grid spacing of 3 km is deemed sufficient to capture the microphysical characters of the two examined IOPs. The vertical distribution of precipitating particles shows differences between IOP2b and IOP8 (Figs. 6–7) for all schemes. Only G2 correctly differentiates the amount of graupel in the two cases, but still overestimates it in IOP8. Gross similarities in the vertical distribution of hydrometeors are also detected by radar observations (Medina and Houze 2003), which show for both events the presence of a deep layer

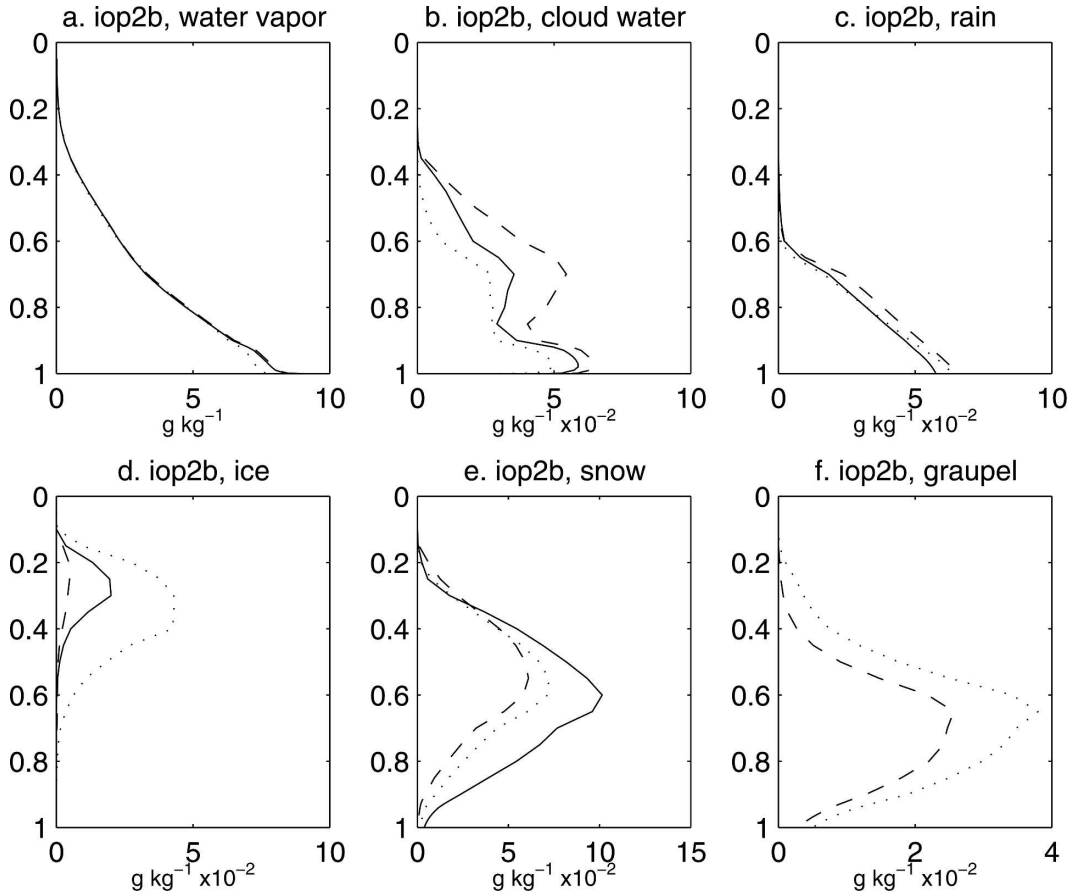

FIG. 6. Averaged vertical profiles of various hydrometeors for IOP2b; R1CNTR (continuous lines), R2 (dashed lines), and G (dotted lines). The profiles were built averaging the mixing ratios over the whole duration of the model run, and over the whole domain 3. The vertical coordinate is the model σ level ($\sigma = 0$ at the model top; $\sigma = 1$ at the surface).

of dry snow above a layer of wet snow (Medina and Houze 2003, their Figs. 12 and 14), although at a different altitude in two cases, because of the different altitude of the 0°C isotherm. A relevant difference between the two events nevertheless exists, and it consists of the occasional occurrence of convective cells with high graupel concentrations in IOP2b, which is instead not observed in IOP8. Although MM5 correctly reproduces the occurrence of convection (Rotunno and Ferretti 2003) and the high graupel concentration in IOP2b, the maximum mixing ratio of graupel is indeed too large in IOP8. This supports the hypothesis that the production of graupel in the bulk microphysical schemes analyzed here largely depends on the thermal structure of the atmosphere more than on the simulated convection; in fact, graupel particles are also produced in events where the 0°C isotherm is shallow (as in IOP8).

A further difference between the microphysical simulations of the two events is found for the vertical position of the maxima: the maximum for any hydrometeor is always located at a slightly higher level for IOP2 than for IOP8. This feature also agrees with measurements by a polarimetric radar, reported by Medina and Houze (2003), and it would suggest enhanced upward vertical motions, which is consistent with the ideal model proposed by Medina and Houze (2003). Another discrepancy in the model results is found in the shape of the cloud water profile: much more cloud water is produced at lower levels for IOP2 than for IOP8. These two latter features are very likely related to different meteorological conditions for the two episodes, but all of the remaining results support the conclusion that complex microphysical parameterization schemes, beyond being inefficient sometimes in forecasting ground precipitation (as previously demonstrated), still have shortcomings in reproducing some particular features of a realistic distribution of hydrometeors (e.g., the occurrence of graupel).

Comparing the simulations of the same single event

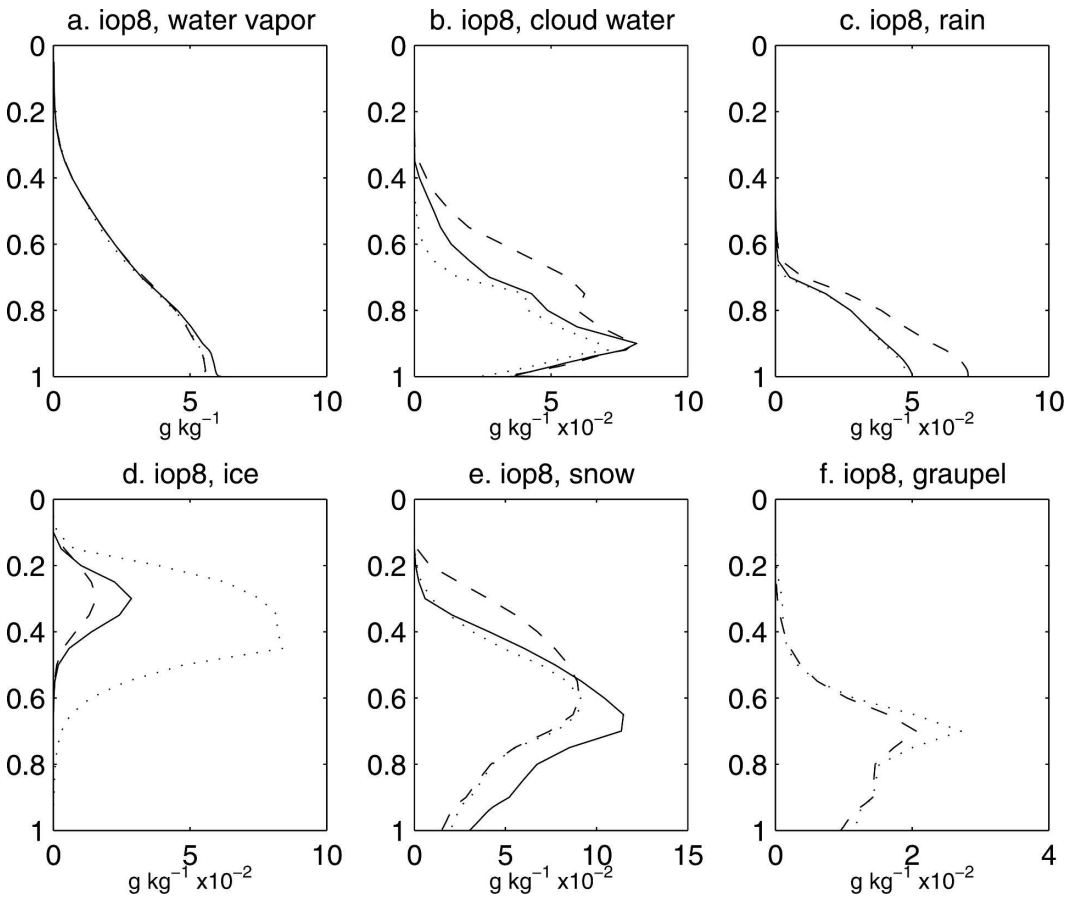

FIG. 7. As in Fig. 6, but for IOP8.

(either IOP2b or IOP8) using different microphysical schemes may lead to some indications about the typical behavior of the schemes themselves. For instance, the R1 scheme produces a larger amount of snow than the others for both IOP2b and IOP8; this feature is partially related to the lack of the graupel water category, which is instead included in both the R2 and G schemes, where it subtracts a certain amount of water mass from the snow-forming processes. Moreover, if G is compared with R2, the former seems to produce higher mixing ratios of ice-phase hydrometeors (snow, graupel, and cloud ice), while the latter is responsible for the production of a greater amount of cloud water and rain at the lower levels. Anyway, it has to be noticed that such differences do not affect significantly the rainfall forecast, as was shown in the previous section by analyzing the verification indices of the different runs. Therefore, the averaged (space and time) reconstruction of microphysical fields does not appear to drastically affect the forecast of surface rainfall. Because of this, the analysis of the features and implications of the modeled vertical distribution of hydrometeors is not carried into further detail in the present study. Although in this study we did not see any remarkable sensitivity to the formulation of microphysical processes, we cannot deny that an accurate knowledge of microphysical parameters and a good ability in reproducing the distribution of hydrometeors may consistently improve the forecast of precipitation.

d. Snowfall speed sensitivity experiments

Colle and Mass (2000) suggested that the snowfall velocity could be a major factor in controlling the amount of precipitation on the windward and lee sides of a mountain ridge. If the fall speed of snow is large, precipitation is favored on the windward side of a ridge, and the air that is blown over the crests is dry; conversely, slow deposition velocities favor the extension of precipitation areas toward the lee side of mountains. In this context, the role of the parameterization of snowfall is thought to be more important than that of rainfall: rain is too heavy and it falls too quickly for its motion to be relevantly affected by wind advection on a regional scale.

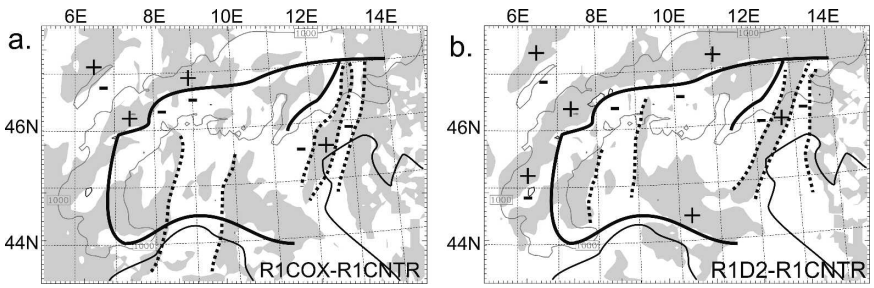

FIG. 8. Differences in daily precipitation using two fall speed parameterizations: (a) R1COX − R1CNTR, and (b) R1D2 − R1CNTR. The white areas indicate higher precipitation for R1CNTR, whereas the gray areas indicate higher precipitation for the test runs; + and − signs correspond to areas with high differences [$\geq$15 mm day^{-1} in (a), and $\geq$40 mm day^{-1} in (b)]. The thick continuous line indicates the mountain ridge of the Alps and Apennines. Dotted lines indicate areas of displacement due to advection of hydrometeors (see text for explanation).

Inaccurate representations of the snowfall velocities can therefore be responsible for relevant location errors in the rainfall forecasts from NWP models. For instance, MM5 is known to often underestimate precipitation on the lee of mountain ridges, and this feature may be related to a flaw in the parameterization of the snowfall speed. Several tests addressing the role of this parameterization have already been made in the northwest Pacific region; recently, Colle et al. (2005) found that a slower fall speed produced 5–15 mm less total precipitation (18-h accumulation) on the windward side of Oregon's Cascade Mountains, and 5–15 mm more on the lee side.

Some numerical experiments are performed here to test the sensitivity of MM5 to the snowfall speed parameterization in the Mediterranean area. The model configuration outlined in section 3 is used to simulate the MAP IOP2b event. The R1 microphysics scheme with the traditional LH parameterization for the snow deposition velocity is taken as the control experiment (R1CNTR). Two sensitivity tests are performed by implementing the C and D2 formulas, R1COX and R1D2, respectively. The former relationship is chosen by analogy with Colle and Mass (2000) and Colle et al. (2005), while the latter is taken because it provides extremely low fall speeds (as shown in Fig. 3), and is thus expected to determine a relevant redistribution of precipitation and a drastically different rainfall field. Other sensitivity tests using the JB1, JB2, and D1 relationships have been performed, but they did not display remarkable differences with the simulations performed using C and LH. Therefore, they will not be shown.

An evaluation of the differences in the forecast of daily precipitation between R1CNTR, R1COX, and R1D2 is provided in Fig. 8. The gray areas (Fig. 8) correspond to regions where the R1COX and R1D2 test runs generate larger precipitation than that of R1CNTR. The location of extreme values in the differences, both positive and negative, is marked by + and − signs. A reduction of the precipitation in the windward slope and an increase in the lee side is found for both R1COX and R1D2, as expected, and the differences are particularly remarkable along the crests of the Alps and Apennines (Fig. 8; the continuous black line indicates the position of the Alpine and Apennines divides).

The maximum difference between the rainfall produced by R1COX and R1CNTR is of approximately $\pm$20 mm (Fig. 8a, 46°N, 13°E), that is, no more than 20% of the observed rainfall. Because the differences between R1COX and R1CNTR are not very large, they do not affect the verification scores of the two simulations as Fig. 9 shows. The ets and bias for R1CNTR and R1COX are approximately equivalent, despite some deviations at high thresholds (approximately 70 mm). These results show a poor sensitivity of the rainfall forecast to the parameterization of the snowfall speed, in contrast to what was found by Colle and Mass (2000), who reported achieving differences between 10 and 70 mm (10%–60% of the observed rainfall) by substituting LH with C, which allowed them to obtain a relevant improvement in the forecast.

The differences between precipitation forecasts from R1D2 and R1CNTR are similar to those between R1COX and R1CNTR, but they are larger in magnitude. R1D2 yields a terminal fall speed that is about 20% as much as that given by LH, and it concentrates much more rainfall on the downwind (northern) slope of the Alps (Fig. 8b). Differences greater than 40 mm in the forecast of daily rainfall are detected in this case; such deviations are also reflected in significant differences in the verification scores. Figure 9 shows that

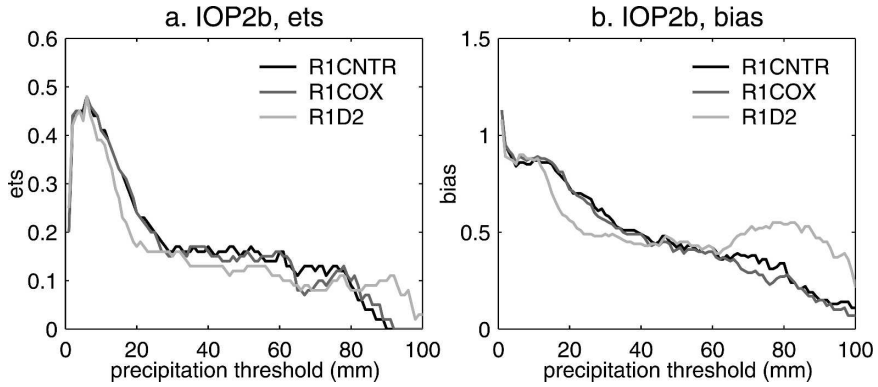

FIG. 9. (a) Ets and (b) bias scores for the IOP2b 12-h accumulated precipitation in domain D2 for R1CNTR, R1COX, and R1D2.

R1D2 produces worse scores at a low precipitation threshold and better scores at high rainfall amounts.

The decrease of the model skill for intermediate rainfall thresholds can be understood considering that the R1D2 experiment is drier than R1CNTR in the Piedmont region and in the plains of northern Italy. Piedmont is on the windward side of the mountain ridge for the IOP2b, and therefore a reduction of precipitation on this side results in worsening the (already too dry) model forecast. Conversely, the improvement in the model performance at high precipitation amounts for R1D2 is related to a favored advection of precipitating particles toward the crest of the Alpine ridge; this results in a larger rainfall rate, which reduces the model bias and increases its forecast skill.

Last, it is worthwhile to notice that in both R1COX and R1D2 the variations in rainfall produced by changing the snowfall speed function are characterized by south-southwest- to north-northeast-oriented bands, especially in the eastern part of domain D2. These are shown in Fig. 8 by dotted black lines. This would suggest some other factor than orography influencing these variations, for example, a different horizontal advection of precipitating particles. Thus, changing the snowfall speed seems to affect the forecast of rainfall in at least the following two ways: 1) controlling the positioning of rainfall on the slopes of a mountain ridge, and 2) affecting the advection of rainbands with the prevalent atmospheric flow.

To better quantify the impact of the different snowfall speed functions on the precipitation forecast, the skill scores for IOP2b are evaluated separately for the lee and windward sides of the mountain ridge by distributing the stations on the opposite slopes of the Alps in two separate datasets. This is achieved by considering the stations in Italy, Slovenia, and southern Switzerland (Ticino) as the "windward" dataset, and those in Austria and northern Switzerland as the "lee" dataset. This choice is driven by the position of the stations with respect to the Alps, and is motivated by the southerly wind in IOP2b being approximately perpendicular to the ridge. Only the results from the R1CNTR, R1COX, and R1D2 are presented.

The ets shows higher values in the windward side than in the lee slope for all snowfall speeds (Figs. 10a–c), suggesting that MM5 has a better skill in predicting precipitation in the south side of the Alpine ridge than in the other one. The bias shows (Figs. 10b–d) that MM5 tends to produce dry forecasts on both sides of the ridge, although the underestimation of precipitation is larger in the upwind slope (where the bias is on average lower than on the lee side). This agrees with previous studies showing that MM5 has higher skill upstream than downstream (Ferretti et al. 2003), and that it fails in forecasting weak and widespread rainfall, as is the case with the precipitation regime north of the Alps in IOP2b.

At intermediate precipitation thresholds, R1CNTR appears to have slightly better scores than the others, upwind of the Alps. In general, if the flow is southerly a reduction of the terminal snowfall velocity produces dry and worse forecasts in northern Italy; R1CNTR is already dry on the windward slope of the Alps, and therefore transferring precipitation to the other slope yields poorer results.

As expected, R1D2 has remarkably different behavior from that of R1CNTR and R1COX; this fall speed formulation transfers a relevant amount of rainfall from the Po Valley plains toward the ridge and the downwind slope of the Alps. As a consequence, the rainfall forecast in the plain area becomes drier than for R1CNTR, while more rain is produced both in the lee dataset and in the mountainous region of the windward dataset (where the observed rainfall is higher than in

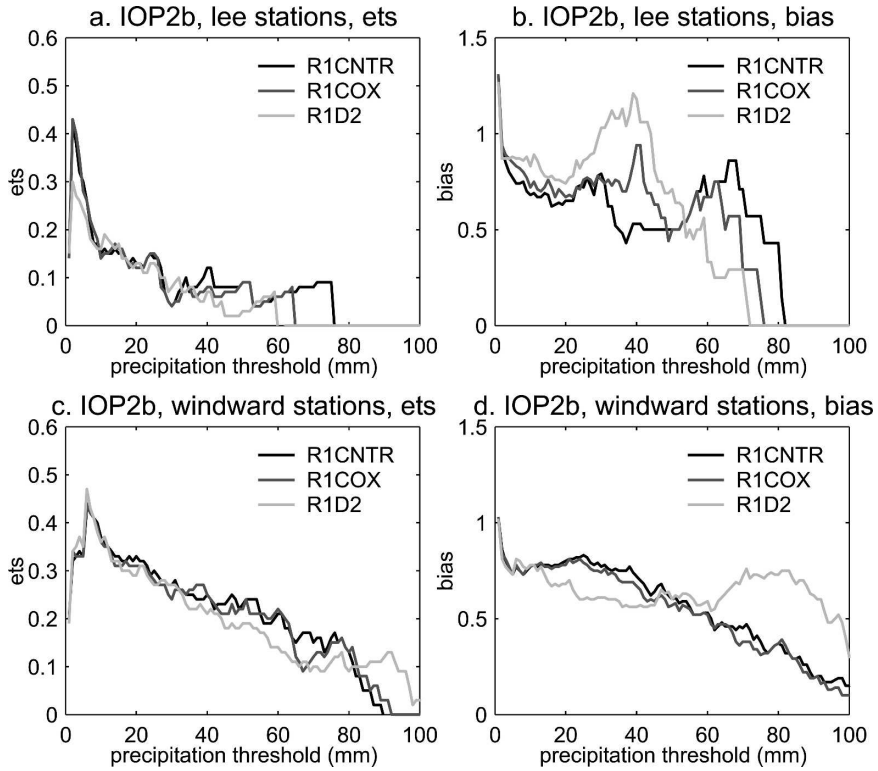

FIG. 10. (a), (c) Ets and (b), (d) bias for the stations in the lee and windward sides of the alpine ridge for R1CNTR, R1COX, and R1D2; 12 h-cumulated precipitation in IOP2b is considered.

the plains). This clearly appears in the verification scores; R1D2 has high bias on the lee side of the Alps up to a 50-mm threshold, and also for the highest rainfall in the windward side (which occurred close to the mountain ridge). Because of the relevant underestimation of precipitation occurring on the plains in the upwind region, the bias score at intermediate rainfall thresholds in the windward dataset becomes worse. It is worthwhile to notice that the improvement for the bias on the lee side brought on by the D2 fall speed function does not result in an analogous improvement for the ets, suggesting that more is needed to improve the accuracy of rainfall forecasting than simply transferring rainfall from one side of a mountain ridge to the other.

A number of case studies representing different environmental conditions would be needed in order to achieve a more precise assessment of how forecasts would be affected by changing the parameterization of the snowfall speed. Nevertheless, the results obtained by analyzing only IOP2b seem to support three general results. First, the fall speed of snow indeed appears to have a significant impact on the forecast of rainfall by an NWP model, but MM5 does show large sensitivity to this parameter only if a very large variation is applied to it. Second, the variations determined by changing the fall speed relationship only result in a redistribution of the modeled rainfall, and do not affect significantly the total rainfall volume in the area under investigation (greater precipitation in a region is always compensated for by smaller precipitation in an adjacent one). Last, the impact of these variations does not appear to affect systematically the skill of the model, whose forecasts can either be improved or made worse depending on their geographical location and on the ongoing atmospheric dynamics.

5. Conclusions

An evaluation of the sensitivity of the rainfall forecasts from MM5 to different bulk microphysical schemes is performed, using two rainfall events in the Mediterranean region as test cases (the MAP events IOP2b and IOP8). Three different microphysics schemes are tested, and the sensitivity of the numerical simulations to different parameterizations of the snowfall speed is also addressed. The results obtained here confirm the overall tendency of MM5 to underestimate rainfall both on the windward and on the lee sides of

mountain ridges, which has already been reported in a number of other investigations.

All microphysical schemes produce very different vertical distributions of hydrometeors in the two IOPs; nevertheless, model simulations fail to reproduce some features highlighted by the observations available from polarimetric radars, in particular concerning the distribution of graupel particles in IOP8. This would suggest that a mesoscale model like MM5 is only partially able to provide a realistic reconstruction of microphysical fields when run at a maximum resolution of 3 km. The simulated rainfall does not show large sensitivity to the different microphysics schemes either at the hourly or at the daily time scale, confirming indications from previous studies, for example, Zängl (2004) and Colle et al. (2005). The inclusion of ice-phase processes only appeared to slightly improve the forecast of rainfall at very high thresholds. These indications result from a quantitative comparison between rain gauge observations and forecasts; therefore, they need to be taken with necessary caution, motivated by the limited representativeness of a precipitation field that can be obtained by such point-wise measurements.

Some experiments have also been performed to assess the sensitivity of rainfall forecasts to different formulations of the parameterization of the deposition velocity of snow. Remarkable impacts, such as large enhancements of the model rainfall on the lee sides of ridges, are only found if a very large reduction of the snowfall speed is applied. Whether this impact positively or negatively affects the overall forecast skill depends on the geographical location and meteorological conditions.

The results obtained here show that a refinement of the microphysical parameterization, for example, a more complete description of ice-phase processes, appears to have a potential for improving the model accuracy. Anyway, the verification analysis performed in this study shows that the effect of such changes on the quality of the rainfall forecasts provided by models in an operational setup is still modest. In contrast, the impact of changes in the snowfall speed formulation is potentially very relevant, but it only leads to a geographical redistribution of the predicted rainfall volumes, rather than to a variation in their magnitude; consequently, such adjustments would only provide a partial correction of errors in the location of rainfall areas, but not of errors in rainfall amount.

Previous studies showed that the large mesoscale dynamical and moisture fields for IOP2b and IOP8 were properly reconstructed by MM5 (Rotunno and Ferretti 2003). Faccani and Ferretti (2005) provided insight about the role of initial conditions in the two cases and about the use of three-dimensional data assimilation techniques to improve most of the model-predicted field, but the precipitation only slightly (Ferretti and Faccani 2005). Further, in this study, the verification of rainfall forecasts using skill scores does not allow any significant effect of microphysical parameterizations on the forecast skill to be highlighted, independent of the ongoing microphysical processes, which are different in IOP2b and IOP8.

On the other hand, several recent studies highlighted the general importance of the representation of diffusion processes in the forecast of rainfall. Both the parameterization of subgrid-scale diffusion in the boundary layer (e.g., Hong and Pan 1996; Zampieri et al. 2005) and the computation of diffusion terms on terrain-following meshes (Zängl 2004) appear to have a large impact on the modeled precipitation. An investigation of the role of these model features in the forecast of rainfall in IOP2b and IOP8 may be the subject of further analysis in the future.

Last, and perhaps surprising, is that microphysical parameterizations appear to have a small impact on the numerical simulations of rainfall performed in this work, if compared with other studies focused on different target areas (e.g., the U.S. Pacific Northwest). We believe that pursuing a better knowledge of microphysical processes and parameters in the Mediterranean region, possibly through an ad hoc campaign, would help in building and tuning better and more effective models.

Acknowledgments. NCAR is acknowledged for MM5. CETEMPS (Prof. Guido Visconti) and Prof. Dino Zardi are gratefully acknowledged for supporting and encouraging this research. ECMWF, the MAP archive, and the ITAMAP group are acknowledged for the data.

REFERENCES

Bougeault, P., and Coauthors, 2001: The MAP Special Observing Period. *Bull. Amer. Meteor. Soc.,* **82,** 433–462.

Brewster, K. A., 2003: Phase-correcting data assimilation and application to storm-scale numerical weather prediction. Part I: Model description and simulation testing. *Mon. Wea. Rev.,* **131,** 480–492.

Colle, B. A., and C. F. Mass, 2000: The 5–9 February 1996 flooding event over the Pacific Northwest: Sensitivity studies and evaluation of the MM5 precipitation forecasts. *Mon. Wea. Rev.,* **128,** 593–617.

——, and Y. Zeng, 2004: Bulk microphysical sensitivities within the MM5 for orographic precipitation. Part II: Impact of barrier width and freezing level. *Mon. Wea. Rev.,* **132,** 2802–2815.

——, K. J. Westrick, and C. F. Mass, 1999: Evaluation of MM5 and Eta-10 precipitation forecasts over the Pacific Northwest during the cool season. *Wea. Forecasting,* **14,** 137–154.

——, M. F. Garvert, J. B. Wolfe, C. F. Mass, and C. P. Woods, 2005: The 13–14 December 2001 IMPROVE-2 event. Part III: Simulated microphysical budgets and sensitivity studies. *J. Atmos. Sci.,* **62,** 3535–3558.

Cox, G., 1988: Modeling precipitation in frontal rainbands. *Quart. J. Roy. Meteor. Soc.,* **114,** 115–127.

Davis, C., 1974: Ph.D. thesis, University of Wyoming, Dept. of Environ. Sci. (as cited in Pruppacher and Klett 1997).

Doswell, C. A., III, C. Ramis, R. Romero, and S. Alonso, 1998: A diagnostic study of three heavy precipitation episodes in the Western Mediterranean region. *Wea. Forecasting,* **13,** 102–124.

Dudhia, J., 1993: A nonhydrostatic version of the Penn State–NCAR Mesoscale Model: Validation tests and simulation of an Atlantic cyclone and cold front. *Mon. Wea. Rev.,* **121,** 1493–1513.

Faccani, C., and R. Ferretti, 2005: Data assimilation of high density observations: Part I. Impact on the initial conditions for the MAP/SOP IOP2b. *Quart. J. Roy. Meteor. Soc.,* **131,** 21–42.

Ferretti, R., and C. Faccani, 2005: Data assimilation of high density observations: Part II. Impact on the forecast of the precipitation for the MAP/SOP IOP2b. *Quart. J. Roy. Meteor. Soc.,* **131,** 43–61.

——, T. Paolucci, G. Giuliani, T. Cherubini, L. Bernardini, and G. Visconti, 2003: Verification of high-resolution real-time forecasts over the Alpine region during the MAP SOP. *Quart. J. Roy. Meteor. Soc.,* **129B,** 587–607.

Fritsch, J., and J. Kain, 1993: Convective parameterization for mesoscale models: The Kain–Fritsch scheme. *The Representation of Cumulus in Numerical Models, Meteor. Monogr.,* No. 46, Amer. Meteor. Soc., 165–177.

Garvert, M. F., C. P. Woods, B. A. Colle, C. F. Mass, P. V. Hobbs, M. T. Stoelinga, and J. B. Wolfe, 2005: The 13–14 December 2001 IMPROVE-2 event. Part II: Comparison of MM5 model simulations of clouds and precipitation with observations. *J. Atmos. Sci.,* **62,** 3520–3534.

Gilmore, M. S., J. M. Straka, and E. N. Rasmussen, 2004: Precipitation and evolution sensitivity in simulated deep convective storms: Comparisons between liquid-only and simple ice and liquid phase microphysics. *Mon. Wea. Rev.,* **132,** 1897–1916.

Grell, G., J. Dudhia, and D. Stauffer, 1994: A description of the fifth-generation Penn State/NCAR Mesoscale Model (MM5). NCAR Tech. Rep. NCAR/TN-389+IA, 122 pp.

Hong, S.-Y., and H.-L. Pan, 1996: Nonlocal boundary layer vertical diffusion in a medium-range forecast model. *Mon. Wea. Rev.,* **124,** 2322–2339.

Jiusto, J., and G. Bosworth, 1971: Fall velocity of snowflakes. *J. Appl. Meteor.,* **10,** 1352–1354.

Jolliffe, I. T., and D. B. Stephenson, Eds., 2004: *Forecast verification: A Practitioner's Guide in Atmospheric Science*. John Wiley and Sons, 254 pp.

Locatelli, J., and P. Hobbs, 1974: Fall speeds and masses of solid precipitation particles. *J. Geophys. Res.,* **79,** 2185–2197.

Lynn, B. H., A. P. Khain, J. Dudhia, D. Rosenfeld, A. Pokrovsky, and A. Seifert, 2005a: Spectral (bin) microphysics coupled with a mesoscale model (MM5). Part I: Model description and first results. *Mon. Wea. Rev.,* **133,** 44–58.

——, ——, ——, ——, ——, and ——, 2005b: Spectral (bin) microphysics coupled with a mesoscale model (MM5). Part II: Simulation of a CaPE rain event with a squall line. *Mon. Wea. Rev.,* **133,** 59–71.

Marshall, J., and W. Palmer, 1948: The distribution of raindrops with size. *J. Meteor.,* **5,** 165–166.

Medina, S., and R. A. Houze, 2003: Airmotions and precipitation growth in alpine storms. *Quart. J. Roy. Meteor. Soc.,* **129B,** 342–372.

——, B. F. Smull, and R. A. Houze, 2005: Cross-barrier flow during orographic precipitation events: Results from MAP and IMPROVE. *J. Atmos. Sci.,* **62,** 3580–3598.

Pruppacher, H. R., and J. D. Klett, 1997: *Microphysics of Clouds and Precipitation*. 2d ed. Kluwer Academic, 954 pp.

Reisner, J., R. Rasmussen, and R. Bruintjes, 1998: Explicit forecasting of supercooled liquid water in winter storms using the MM5 mesoscale model. *Quart. J. Roy. Meteor. Soc.,* **124,** 1071–1107.

Richard, E., N. Asencio, R. Benoit, A. Buzzi, R. Ferretti, P. Malguzzi, S. Serafin, G. Zängl, and J.-F. Georgis, 2002: Intercomparison of the simulated precipitation fields of the MAP/IOP2b with different high-resolution models. *Proc. 10th Conf. on Mountain Meteorology and MAP Meeting,* Park City, UT, Amer. Meteor. Soc., 167–170.

Rotunno, R., and R. Ferretti, 2003: Orographic effects on rainfall in MAP cases IOP2b and IOP8. *Quart. J. Roy. Meteor. Soc.,* **129B,** 373–390.

Stoelinga, M. T., and Coauthors, 2003: Improvement of Microphysical Parameterization through Observational Verification Experiment (IMPROVE). *Bull. Amer. Meteor. Soc.,* **84,** 1807–1826.

Tao, W.-K., and J. Simpson, 1993: Goddard cumulus ensemble model. Part I: Model description. *Terr. Atmos. Oceanic Sci.,* **4,** 35–72.

Thompson, G., R. M. Rasmussen, and K. Manning, 2004: Explicit forecasts of winter precipitation using an improved bulk microphysics scheme. Part I: Description and sensitivity analysis. *Mon. Wea. Rev.,* **132,** 519–542.

Wilks, D. S., 1995: *Statistical Methods in the Atmospheric Sciences. An Introduction*. Academic Press, 467 pp.

Zampieri, M., P. Malguzzi, and A. Buzzi, 2005: Sensitivity of quantitative precipitation forecasts to boundary layer parameterization: A flash flood case study in the Western Mediterranean. *Nat. Hazards Earth Syst. Sci.,* **5,** 603–612.

Zängl, G., 2004: The sensitivity of simulated orographic precipitation to model components other than cloud microphysics. *Quart. J. Roy. Meteor. Soc.,* **130,** 1857–1875.